Redox Reactions of Copper Complexes Formed with Different β-Amyloid Peptides and Their Neuropathalogical Relevance†

Dianlu Jiang,‡ Lijie Men,§ Jianxiu Wang,‡ Yi Zhang,‡ Sara Chickenyen,‡ Yinsheng Wang,§ and Feimeng Zhou*,‡

Department of Chemistry and Biochemistry, California State University, Los Angeles, Los Angeles, California 90032, and Department of Chemistry, University of California at Riverside, Riverside, California 92521

Received March 13, 2007; Revised Manuscript Received June 4, 2007

ABSTRACT: The binding stoichiometry between Cu(II) and the full-length β-amyloid Aβ(1−42) and the oxidation state of copper in the resultant complex were determined by electrospray ionization−Fourier transform ion cyclotron resonance mass spectrometry (ESI-FTICR-MS) and cyclic voltammetry. The same approach was extended to the copper complexes of Aβ(1−16) and Aβ(1−28). A stoichiometric ratio of 1:1 was directly observed, and the oxidation state of copper was deduced to be 2+ for all of the complexes, and residues tyrosine-10 and methionine-35 are not oxidized in the Aβ(1−42)−Cu(II) complex. The stoichiometric ratio remains the same in the presence of more than a 10-fold excess of Cu(II). Redox potentials of the sole tyrosine residue and the Cu(II) center were determined to be ca. 0.75 and 0.08 V vs Ag/AgCl [or 0.95 and 0.28 V vs normal hydrogen electrode (NHE)], respectively. More importantly, for the first time, the Aβ−Cu(I) complex has been generated electrochemically and was found to catalyze the reduction of oxygen to produce hydrogen peroxide. The voltammetric behaviors of the three Aβ segments suggest that diffusion of oxygen to the metal center can be affected by the length and hydrophobicity of the Aβ peptide. The determination and assignment of the redox potentials clarify some misconceptions in the redox reactions involving Aβ and provide new insight into the possible roles of redox metal ions in the Alzheimer's disease (AD) pathogenesis. In cellular environments, the reduction potential of the Aβ−Cu(II) complex is sufficiently high to react with antioxidants (e.g., ascorbic acid) and cellular redox buffers (e.g., glutathione), and the Aβ−Cu(I) complex produced could subsequently reduce oxygen to form hydrogen peroxide via a catalytic cycle. Using voltammetry, the Aβ−Cu(II) complex formed in solution was found to be readily reduced by ascorbic acid. Hydrogen peroxide produced, in addition to its role in damaging DNA, protein, and lipid molecules, can also be involved in the further consumption of antioxidants, causing their depletion in neurons and eventually damaging the neuronal defense system. Another possibility is that Aβ−Cu(II) could react with species involved in the cascade of electron transfer events of mitochondria and might potentially sidetrack the electron transfer processes in the respiratory chain, leading to mitochondrial dysfunction.

Alzheimer's disease (AD)[1] is a progressive neurodegenerative disorder underscored by the appearance of senile plaques in disease-inflicted brains. The major components in senile plaques are peptides containing 39−43 amino acid residues (amyloid-β or Aβ peptides) generated from proteolytic cleavage of the amyloid precursor protein (APP) by β- and γ-secretases (*1*, *2*). Such findings (*2*, *3*) led to the hypothesis that deposition of Aβ fibrils and other aggregates is responsible for neuronal cell loss (*4*). However, how β-amyloid associates with the AD pathogenesis remains unclear.

Other characteristics in AD-affected brains include the enhanced level of oxidative stress manifested by extensive oxidation of proteins (*5*−*7*) and DNA (*8*−*10*), unusually high levels of metals (e.g., copper, zinc, and iron) present in the senile plaques, and a decline of polyunsaturated fatty acids (*11*, *12*) coupled with increased lipid peroxidation (*13*−*15*). On the basis of the amyloid hypothesis and the existence of oxidative stress, Butterfield and co-workers (*15*) proposed a model to account for neurodegeneration in AD, viz., β-amyloid peptide-initiated oxidative stress and neurotoxicity. The aggregated amyloid peptide, perhaps in concert with complexed redox metal ions, produces free radicals and triggers a cascade of events, which include, but are not limited to, protein oxidation, lipid peroxidation, and cellular dysfunction. All of these detrimental processes result in death of neurons (*15*).

Together with these pathological characteristics, intracellular lesions, including impairment of mitochondrial energy metabolism, have also been purported to be a cause of the

† This work was supported by NIH research grants (Grant GM 08101 to F.Z. and Grant R01 CA101864 to Y.W.) and partially supported by the NIH-RIMI Program at California State University, Los Angeles (P20 MD001824-01).

* Corresponding author. Phone: 323-343-2390. Fax: 323-343-6490. E-mail: fzhou@calstatela.edu.

‡ California State University, Los Angeles.

§ University of California at Riverside.

[1] Abbreviations: AD, Alzheimer's disease; Aβ, β-amyloid; ADHP, 10-acetyl-3,7-dihydroxyphenoxazine; APP, amyloid precursor protein; CV, cyclic voltammetry; ESI-FTICR-MS, electrospray ionization−Fourier transform ion cyclotron mass spectrometry; ET, electron transfer; Met-35, methionine at position 35; MS, mass spectrometry; ROS, reactive oxygen species; Tyr-10, tyrosine at position 10.

10.1021/bi700508n CCC: $37.00
Published on Web 07/18/2007

AD development (*9*, *10*, *16*, *17*). In addition, impaired energy metabolism and altered cytochrome *c* oxidase activity are among the earliest detectable defects in AD (*18*−*21*). Recently, the linkage between mitochondrial dysfunction and Aβ peptides has been suggested by Deshpande et al. (*22*), who showed that, after treatment of neuronal cells with Aβ oligomers, mitochondrial redox potential dropped precipitously. A marked decease in ATP level and drastic increases in caspase activation and lactate dehydrogenase (LDH) release were also observed prior to the occurrence of massive cell death (*22*). It also has been reported that synthetic Aβ inhibited activity of the human cytochrome *c* oxidase and the inhibitory effect is dependent on the copper content (*23*, *24*). Only in the presence of copper does Aβ significantly inhibit the activity of human cytochrome *c* oxidase in mitochondria. These results suggest that copper plays a significant role in the neurotoxicity of Aβ.

The brain utilizes metal ions for many biochemical reactions, and cortical neurons release exchangeable copper and zinc ions during depolarization and neurotransmission (*25*, *26*). Whether metal ions are involved in the pathogenesis of AD and what roles they play in the evolvement of oxidative stress and AD development are not known. Yet, the fact that senile plaques in the neocortical region of the brains of AD patients contain up to millimolar concentrations of Zn^{2+}, Cu^{2+}, and Fe^{3+} (*27*) suggests that metal ions probably play a pivotal role in the generation of reactive oxygen species (ROS). A recent study by Raman spectroscopy of senile plaques extracted from postmortem samples demonstrated that copper and zinc ions are bound via histidine imidazole rings (*28*). More importantly, it was found that extensive methionine oxidation in Aβ has occurred in intact plaques (*28*). For metals to exert important influences on the AD pathogenesis, it is likely that a series of redox reactions facilitated by the metal-containing Aβ species have occurred, leading to the production of ROS and/or the interruption of the electron transfer (ET) chain in the respiratory processes. Along this line, Cu(II) coordination with Aβ has been extensively investigated (*29*−*34*). In support of the important role of copper-containing Aβ species in ROS production, studies have shown that in vitro incubation of an Aβ/Cu(II) mixture with electron donors under aerobic condition produced hydrogen peroxide (*35*−*37*).

A number of techniques have been employed for examining the various aspects of the interactions between β-amyloid and copper ions (e.g., the structure of and binding sites in the complex) (*34*, *35*, *38*, *39*). Although conflicting results have been reported on certain aspects (for example, the metal binding stoichiometry and affinity) (*29*, *34*, *38*, *39*), it is generally accepted that metal ions are bound to the hydrophilic portion of Aβ species (residues 1−16). Moreover, the involvement of histidine residues at positions 6, 13, and 14 has been ascertained by many studies (*30*, *34*, *38*). Given the wide existence of ET processes in cells in general and neuronal cells in particular, the introduction of exogenous redox-active species may alter the ET reactions or pathways in mitochondria. The accurate determination of redox potentials of Aβ and its metal complexes will certainly help to unravel their roles in oxidative stress, metal homeostasis and detoxification, and Aβ aggregation/fibrillation. Surprisingly, other than a single experiment comparing the voltammetric behaviors of Aβ(1−42) and its copper complex (*35*), a systematic effort has not been made to measure accurately the redox potentials of metal complexes of the full-length and different segments of Aβ and to relate them to redox reactions in cellular milieu. Moreover, there exist inconsistencies in the interpretations of the redox reactions of the Aβ−metal complexes (e.g., whether Cu(II) can be reduced by Aβ and, if the reduction does occur, which constituents in Aβ cause the reduction) (*27*, *35*, *37*, *40*). Compounded by the complexity in Aβ structural elucidation and the possible involvement of Aβ in many cellular processes, evidence regarding the effect of redox-active metal ions on ROS generation and the possible oxidations of the methionine residue near the C terminus (Met-35) and the tyrosine moiety in the hydrophilic domain (Tyr-10) remain either indirect or largely elusive.

Electrochemical methods can allow for the accurate and direct determination of potentials of redox-active biomolecules and provide insight about their ET reactions (*41*). By judiciously choosing the electrode materials and electrolyte system, one can achieve facile ET rates at the electrode/solution interface and reliably determine the redox potentials. In this study, we employed cyclic voltammetry (CV) and mass spectrometry (MS) to investigate the redox properties of several Aβ variants and their copper complexes. We present strong evidence about the inability of Aβ, in the absence of a cofactor (i.e., a reductant), to reduce Cu(II) and report on an experiment in which the electrogenerated Aβ−Cu(I) complex can indeed facilitate the catalytic reduction of dissolved oxygen to hydrogen peroxide. On the basis of the redox potential of Aβ−Cu(II) and comparison of it to those of selected cellular reductants, the implications of the Aβ involvement in the production of ROS and the ET chain of mitochondria and their relations with AD pathogenesis are discussed.

MATERIALS AND METHODS

Materials. Lyophilized Aβ(1−16), Aβ(1−28), and Aβ(1−42) (DAEFRHDSGYEVHHQK^{16}LVFFAEDVGSNK^{28}GAIIGLMVGGVVIA^{42}) samples were purchased from American Peptide Co. Inc. (Sunnyvale, CA). Aβ(1−28) and Aβ(1−42) samples, generously provided by Prof. C. Glabe (University of California at Irvine, CA), were also used in this study. No difference in terms of experimental results between the two sources of Aβ samples was found. Other chemicals were of analytical grade (Sigma-Aldrich). All of the aqueous solutions were prepared using Millipore water (18 MΩ cm). Throughout the work, 1 mM $CuCl_2$ dissolved in 1 mM H_2SO_4 was used as the Cu(II) stock solution. Aβ(1−16) were prepared freshly by dissolving lyophilized powder samples in Millipore water or 5 mM NaOH. No apparent difference was observed for electrochemistry and MS results between samples dissolved in water and those dissolved in NaOH. To ensure no substantial aggregation occurs and to rid the solution of any aggregates, Aβ(1−28) and Aβ(1−42) samples were routinely prepared using a similar protocol developed by Teplow and co-workers (*42*) and Zorgowski and co-workers (*43*). Briefly, Aβ stock solutions (0.5 mM) were prepared daily by dissolving the lyophilized Aβ in 5 mM NaOH. This was followed by sonication for 1 min. The as-prepared solutions were centrifuged at 13000 rpm for 30 min, and the supernatants

were pipetted out for further dilutions. During the relatively short voltammetric and MS measurements, Aβ(1−16) and Aβ(1−28) were not found by atomic force microscopy to aggregate considerably, whereas small amounts of oligomers of Aβ(1−42) were observed. By decreasing the Aβ(1−28) concentration and adding 10% dimethyl sulfoxide (DMSO) into the Aβ(1−42) solution, aggregation in both cases was avoided or significantly retarded.

Electrochemical Measurements. All of the electrochemical experiments were performed on a CHI 832 electrochemical workstation (CH Instruments, Austin, TX) using a homemade plastic electrochemical cell. A glassy carbon disk electrode and a platinum wire were used as the working and counter electrodes, respectively. The reference electrode was Ag/AgCl, and all of the potential values are reported with respect to this electrode unless otherwise stated. Prior to each experiment, the glassy carbon electrode was polished with diamond pastes of 15 and 3 μm and alumina pastes of 1 and 0.3 μm in diameter (Buehler, Lake Bluff, IL). The electrolyte solution was a 10 mM phosphate buffer (pH 7.4) containing 0.1 M Na_2SO_4. Although it has been noted that different buffer solutions may affect Aβ−Cu(II) binding and the subsequent H_2O_2 generation, we did not test other buffers because H_2O_2 had been detected in phosphate buffer containing Aβ and Cu(II) (*37*). Thus, the voltammetric studies in such an electrolyte solution are more relevant to the elucidation of the redox reactions of Aβ−Cu(II) and H_2O_2 generation. For Aβ(1−16) and Aβ(1−28), aliquots of Aβ from stock solutions were diluted with the phosphate buffer to desired concentrations. For voltammetric studies in the presence of Cu(II), these Aβ solutions were spiked with the Cu(II) stock solution to different Aβ/Cu(II) molar ratios. For voltammetric studies of Aβ(1−42), the same procedures were employed except that the 10 mM phosphate/0.1 M Na_2SO_4 (pH 7.4) solution containing 10% dimethyl sulfoxide was chosen to retard the rapid aggregation of Aβ(1−42).

Detection of Hydrogen Peroxide. On the basis of the voltammetric data (cf. Results section), the electrode potential was held at 0.07 V to reduce the Aβ−Cu(II) complex. Possible H_2O_2 generation was monitored using the Fluoro H_2O_2 detection kit (Cell Technology Inc., Mountain View, CA). In the presence of H_2O_2, 10-acetyl-3,7-dihydroxyphenoxazine (ADHP) is oxidized to a fluorescent product, resorufin. This reaction is rapidly catalyzed by peroxidase in a homogeneous solution. Briefly, 50 μL of the sample solution was added to a 50 μL aliquot of the reaction cocktail, which contained 100 μL of 10 mM ADHP, 200 μL of 10 units/mL horseradish peroxidase, and 4.7 mL of reaction buffer. The mixture was then incubated at room temperature in the dark for 10 min. Subsequently, the fluorescence intensity of resorufin was measured at an excitation wavelength of 550 nm with a Cary Eclipse spectrofluorometer (Varian, Inc., Palo Alto, CA). By comparing the fluorescence intensity of resorufin of the sample solution to that of the control, H_2O_2 can be detected.

Electrospray Ionization−Fourier Transform Ion Cyclotron Mass Spectrometry (ESI-FTICR-MS). The ESI-FTICR-MS experiments were conducted on an IonSpec FT-ICR mass spectrometer equipped with a 4.7 T superconducting magnet (IonSpec Inc., Lake Forest, CA) and an LTQ linear ion trap mass spectrometer (Thermo Fisher Scientific, San Jose, CA) operated in the high-resolution, "ultra zoom scan" mode. For the MS measurements, Aβ was first dissolved in a water/methanol solution (50/50 v/v ratio) to yield a 50 μM Aβ stock solution. Aliquots were then diluted with the water/methanol solution to a final concentration of 5 μM. The Aβ solution and Aβ solution spiked with $CuCl_2$ at different molar ratios were introduced to and analyzed by MS. The typical mass resolving power for the FTICR-MS is approximately 200000.

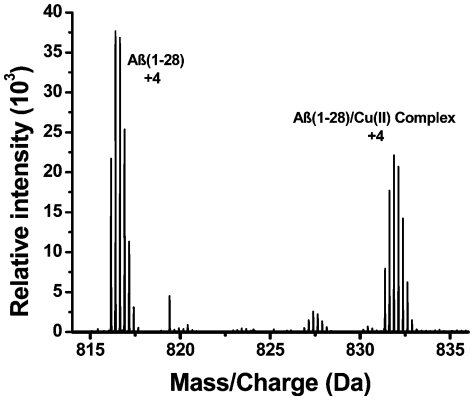

FIGURE 1: Positive-ion ESI-MS of an Aβ(1−28)−Cu(II) mixture at 1:1 ratio.

RESULTS

Copper Binds Aβ at a 1:1 Molar Ratio and the Oxidation State of Copper Is 2+. The coordination chemistry between Cu(II) and Aβ has been investigated by various techniques, such as circular dichroism (CD) spectroscopy (*34*, *35*), electron spin resonance (ESR) (*34*, *35*, *38*), and nuclear magnetic resonance (NMR) (*34*, *39*). While all of the studies indicate that Cu(II) can be incorporated mainly in the hydrophilic domain (residues 1−16), contradictory results have been reported regarding the coordination stoichiometry, the ligands involved, and the oxidation state of copper. A few papers suggested that the Aβ−Cu(II) binding ratio is 1:2 (*29*, *34*), whereas other papers showed that the ratio should be 1:1 (*38*, *39*). MS can provide evidence for the number of copper ions bound per Aβ molecule. ESI-MS is particularly advantageous in that the soft ionization by ESI generates multiply charged species of proteins or peptides while keeping the molecular ions intact. Formation of multiply charged species also decreases the mass-to-charge ratios, shifting molecular ions of large biomolecules to the mass range readily accessible by most mass analyzers (*44*). Furthermore, when the MS employed has a high resolving power, the analysis of isotopic peaks affords an opportunity to deduce the oxidation state of the ligated metal ion. To our knowledge, the use of ESI coupled with high-resolution MS to study Aβ-metal ion binding has not been reported.

The predominant peaks in the ESI-FTICR mass spectra indicate that Aβ and its copper complex are of the 3+, 4+, and 5+ charge states, with the 4+ charge state being the most abundant. Figure 1 shows the *m*/*z* range covering the peaks corresponding to the 4+ charge states of free Aβ(1−28) and its copper complex. Clustered around *m*/*z* 816 and *m*/*z* 832 are the various isotopic peaks of the quadruply charged Aβ(1−28) and Aβ(1−28)−copper ion complex, respectively. An ESI-FTICR mass spectrum of Aβ(1−28) in the absence of Cu^{2+} exhibited peaks around *m*/*z* 816 (see Figure S1 in the Supporting Information). The difference in

Table 1: Extracting the Copper Oxidation State from Mass Peaks of the Aβ(1−28)−Cu(II) Adduct

				Aβ−Cu(I)			Aβ−Cu(II)		
Aβ(1−28)−Cu		measd *m/z*	measd rel abundance (%)	calcd *m/z*	calcd rel abundance (%)	dev (ppm)	calcd *m/z*	calcd rel abundance (%)	dev (ppm)
3+ ion	A	1108.145	15	1108.491	48	310	1108.155	48	9
	A + 1	1108.475	77	1108.825	85	320	1108.489	85	13
	A + 2	1108.806	100	1109.159	100	320	1108.823	100	15
	A + 3	1109.139	75	1109.493	88	320	1109.157	88	16
	A + 4	1109.470	30	1109.827	61	320	1109.491	61	19
4+ ion	A	831.387	36	831.620	48	280	831.368	48	23
	A + 1	831.634	80	831.871	85	280	831.619	85	18
	A + 2	831.883	100	832.121	100	290	831.869	100	17
	A + 3	832.134	93	832.372	88	290	832.120	88	17
	A + 4	832.382	64	832.622	61	290	832.370	61	15
	A + 5	832.634	28	832.872	33	290	832.620	33	17

the mass between the monoisotopic peaks of free Aβ(1−28) and the Aβ(1−28)−Cu complex is 4(831.387 − 816.142) = 60.980 Da. Since the monoisotopic Aβ(1−28)−Cu(II) complex has two less protons, the actual mass difference is 60.980 + 2 = 62.980, which is close to the nominal mass of a copper ion. Therefore, the ESI-MS result supports that the binding stoichiometry between Aβ(1−28) and Cu is 1:1. Further increasing the molar ratio between Cu(II) and Aβ-(1−28) (up to 10) in the solution only changed the relative intensities of the free Aβ(1−28) and Aβ(1−28)−Cu(II) peaks but did not create other peaks of different binding stoichiometries (e.g., 1:2 or 2:1).

The oxidation number of the copper ion in the complex can be determined from the measured *m/z* values of the 4+ ion of the complex. In this respect, if Cu(I) is involved in the formation of the complex, the complex will need to be associated with three protons to yield a 4+ ion; on the other hand, if Cu(II) is present in the complex, it would only require two protons to give a quadruply charged ion. The oxidation number of copper ion present in the complex can, therefore, be determined by comparing the experimentally measured *m/z* values of the isotope clusters for the quadruply charged complex with the calculated *m/z* values for the complexes that are associated with either Cu(I) or Cu(II) (see Table 1). Clearly, the deviations between the measured and calculated *m/z* values for the Cu(II) complex are 15−23 ppm, which are markedly smaller than the 280−290 ppm deviations found for the differences between the measured and calculated *m/z* values for the Cu(I) complex. These results, therefore, strongly support that the charge state of the copper ion in the Aβ(1−28)−copper complex is 2+. Similar analysis of the isotope cluster peaks for the 3+ ion leads to the same conclusion (Table 1).

It has been proposed that Cu(II), in the presence of dissolved oxygen, could alter the redox state of Aβ(1−42), possibly by oxidizing Met-35 into its sulfoxide or sulfone analogues (*30*, *35*, *36*). Thus, since Aβ(1−28) does not comprise the methionine residue, it is conceivable that Cu-(II) remains unchanged upon binding to Aβ(1−28). However, there has been a lack of direct spectroscopic evidence for chemical modifications of methionine even in Aβ(1−42) [except for samples produced under extreme conditions such as laser photolysis (*45*) or from autopsy (*28*)]. It has been further contended that Met-35 oxidation could change the Cu(II) center to Cu(I), which remains coordinated by Aβ-(1−42) (*28*, *35*). If the methionine residue were chemically modified or the copper ion oxidation state were changed,

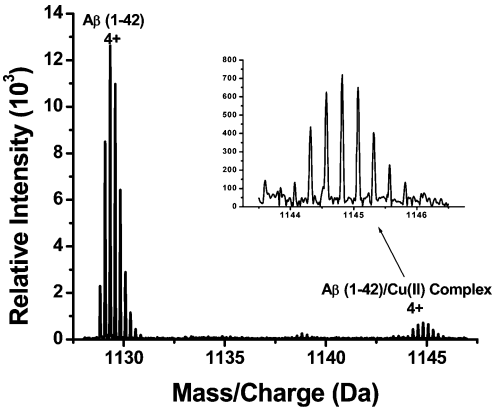

FIGURE 2: Positive-ion ESI-MS of an Aβ(1−42)−Cu(II) mixture at 1:1 ratio.

the mass spectra of Aβ(1−42) treated with Cu(II) would contain peaks showing the addition of oxygen or different *m/z* values for the isotope clusters (vide supra).

To verify whether the ligated Cu(II) could oxidize methionine, we collected mass spectra by spraying a solution containing Aβ(1−42) and Cu(II). Figure 2 is a representative mass spectrum in the mass range encompassing the 4+ charge states of Aβ(1−42) and the Aβ(1−42)−copper ion complex. In Figure 2, peaks corresponding to both free Aβ-(1−42) and the Aβ(1−42)−Cu(II) complex were observed, but any peaks associated with oxidized Aβ(1−42) were absent. This observation strongly suggests that, under the present experimental conditions, Aβ(1−42) itself cannot be oxidized by Cu(II). This observation is further supported by our voltammetric data (vide infra). A detailed analysis of the positions of the peaks corresponding to the 4+ and 5+ charge states again indicates that Cu(II) was not reduced (Table 2), consistent with the fact that the methionine residue was not chemically modified. Our results are also in good agreement with the report from the Zagorski group, who conducted NMR measurements of Aβ(1−40) in the presence of Cu(II) and demonstrated that Met-35 oxidation and Cu-(II) reduction did not occur (*39*). We conducted two additional experiments to show that the Aβ(1−42)−Cu(II) complex is indeed formed by mixing Cu(II) with Aβ(1−42). First, an FT-ICR mass spectrum collected from spraying a solution containing Aβ(1−42) did not exhibit peaks around *m/z* 1145 (Figure S2), indicating that Aβ(1−42)−Cu(II) does not exist in the absence of Cu(II). The second experiment involves the confirmation of the Aβ(1−42)−Cu(II) complex

Table 2: Extracting the Copper Oxidation State from the Measured *m/z* Values of the Aβ(1−42)−Cu(II) Adduct

				Aβ−Cu(I)			Aβ−Cu(II)		
Aβ(1−42)−Cu		measd *m/z*	measd rel abundance (%)	calcd *m/z*	calcd rel abundance (%)	dev (ppm)	calcd *m/z*	calcd rel abundance (%)	dev (ppm)
4+ ion	A	1144.068	19	1144.306	25	210	1144.054	25	12
	A + 1	1144.317	62	1144.556	62	210	1144.304	62	11
	A + 2	1144.568	87	1144.807	92	210	1144.555	92	11
	A + 3	1144.818	100	1145.057	100	210	1144.805	100	11
	A + 4	1145.069	91	1145.308	87	210	1145.056	87	12
	A + 5	1145.318	56	1145.558	62	210	1145.306	62	11
	A + 6	1145.569	31	1145.809	37	210	1145.557	37	11
	A + 7	1145.819	19	1146.059	20	210	1145.807	20	10
5+ ion	A	915.457	32	915.646	25	210	915.444	25	14
	A + 1	915.656	54	915.847	62	210	915.645	62	12
	A + 2	915.856	83	916.047	92	210	915.856	92	12
	A + 3	915.055	100	916.247	100	210	916.046	100	10
	A + 4	916.256	94	916.448	87	210	916.246	87	11
	A + 5	916.456	66	916.648	62	210	916.446	62	11
	A + 6	916.656	40	916.848	37	210	916.647	37	10
	A + 7	916.859	23	916.049	20	210	916.847	20	12
	A + 8	917.063	10	916.249	9	200	917.048	9	16

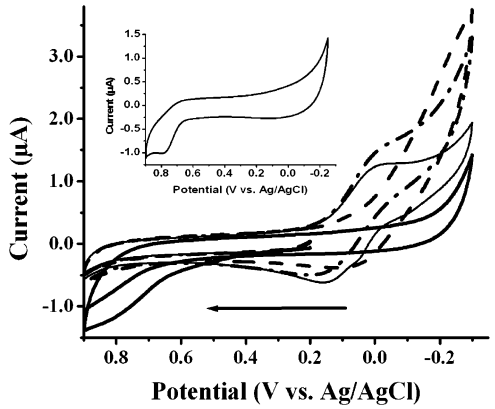

FIGURE 3: Cyclic voltammograms of 200 μM Aβ(1−16) (thick solid curve), 100 μM Cu(II) (dashed curve), a mixture containing 200 μM Aβ(1−16) and 200 μM Cu(II) (thin solid curve), and an O_2-saturated Aβ(1−16)−Cu(II) mixture (dash-dot-dash curve). A voltammogram from a 50 μM tyrosine solution is shown in the inset. All solutions were prepared with a buffer containing 5 mM phosphate and 0.1 M Na_2SO_4 (pH 7.4), and data were obtained at a glassy carbon disk electrode with a diameter of 3 mm. The scan rate was 20 mV/s, and the arrow indicates the initial scan direction.

peak with ESI-MS measurement on a linear ion trap mass spectrometer. As can be seen in Figure S3 and Table S1 in the Supporting Information section, the peaks around *m/z* 1145 are even more pronounced. Due to the greater mass-resolving power of FTICR-MS and to be consistent in comparing the spectra among various species, we focused mainly on the FT-ICR-MS results.

Redox Potentials of Aβ−Cu(II) Complexes. Since the proposed copper binding sites reside in the 16 amino acid N-terminal segment of Aβ(1−42), we first examined the redox behavior of Aβ(1−16) with or without Cu(II). Figure 3 is an overlay of voltammograms of Aβ(1−16) in a Cu(II)-free solution (thick solid curve), free Cu(II) (dashed curve), and Aβ(1−16) in the presence of an equimolar amount of Cu(II) (thin solid curve). To examine the effect of oxygen on the redox process involving Aβ(1−42), we also bubbled O_2 into the mixture of Cu(II) and Aβ(1−16) and then recorded the voltammogram (dash-dot-dash curve). Notice that the voltammogram of Aβ(1−16) (thick solid curve) is rather different than that of Cu(II) (dashed curve), which produced an irreversible reduction peak starting from around 0.0 V. This peak can be attributed to the catalytic reduction of oxygen by the electrogenerated Cu_2O or CuOH layer (*46*). Due to the presence of a trace amount of oxygen in solution, the follow-up catalytic oxidation of Cu_2O or CuOH prevents Cu_2O or CuOH from being further reduced to Cu(0). Therefore, no copper stripping peak was observed. By thoroughly purging the solution with N_2, a copper stripping peak was observed in the CV (Figure S4). The comparison of the voltammogram of Aβ(1−16)−Cu(II) (thick solid curve in Figure 3) to the Cu(II) reduction voltammogram shows that the reduction current of the Aβ-(1−16)−Cu(II) complex is smaller, even though the concentration of the former is twice as high as that of the latter. This suggests that Cu(II) is complexed, since the Aβ(1−16)−Cu(II) is expected to have a smaller diffusion coefficient. For the mixture of Aβ(1−16) and Cu(II), a pair of quasi-reversible waves (thin solid curve) was observed with an oxidation peak at 0.17 V and a reduction peak at ca. 0.0 V. The peak currents decrease inversely with the Aβ(1−16):Cu(II) molar ratio (Table S2). Apparently, catalytic reduction of O_2 by electrogenerated Cu_2O or CuOH occurs at a different potential (<-0.1 V) than the Aβ(1−16)−Cu-(II) complex. We thus assign this pair of waves to the redox reactions between the Aβ(1−16)−Cu(II) and Aβ(1−16)−Cu(I) complexes and report the reduction potential of Aβ-(1−16)−Cu(II) to be 0.085 V vs Ag/AgCl. We noticed that this potential value is similar to that of histidine-rich peptide−Cu(II) complexes (*46*−*48*). The fact that the reduction peak is higher than the oxidation peak suggests that a catalytic follow-up reduction (*49*) takes place after Aβ(1−16)−Cu(II) is reduced. Another noteworthy point is that the oxidation peak became more pronounced as the potential scan rate is increased (data not shown). Furthermore, in the dash-dot-dash curve of Figure 3 the reduction peak was found to increase at the expense of the oxidation peak, suggesting the catalytic nature of the reaction and the involvement of O_2.

The Aβ(1−16) voltammogram exhibited a small and broad oxidation peak at the anodic side of Figure 3 (ca. 0.78 V). This oxidation peak is irreversible and disappears after the first cycle and was observable even when Cu(II) was present

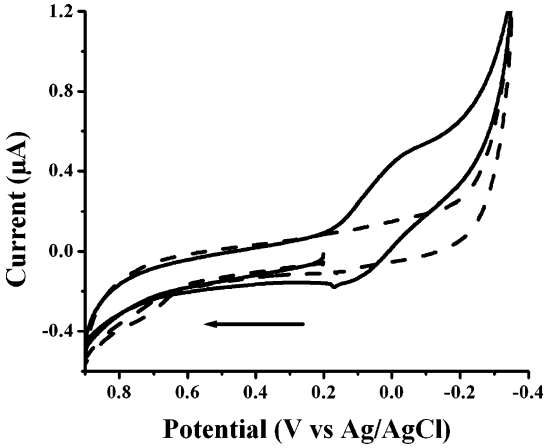

FIGURE 4: Cyclic voltammograms of 50 μM Aβ(1−28) (dashed curve) and a mixture of 50 μM Aβ(1−28) and 50 μM Cu(II) (solid curve) acquired at a glassy carbon disk electrode with a diameter of 3 mm at the scan rate of 20 mV/s. The arrow indicates the scan direction.

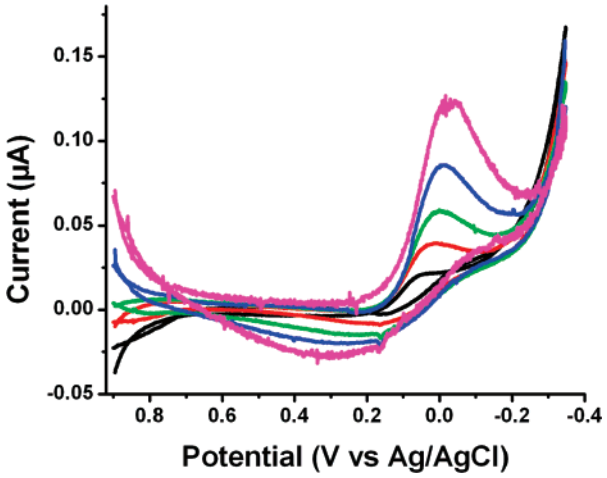

FIGURE 5: Cyclic voltammograms generated by subtracting voltammograms of a 1:1 mixture of Aβ(1−28)−Cu(II) in a N_2-purged solution from those of the same mixture in an air-saturated buffer solution at different scan rates: 0.01 V/s (black), 0.02 V/s (red), 0.04 V/s (green), 0.08 V/s (blue), and 0.16 V/s (purple). A glassy carbon disk electrode with a diameter of 3 mm was used as the working electrode.

(note: the thin solid and dash-dot-dash curves in Figure 3 were acquired during the second cycle). Thus the peak must originate from the oxidation of a segment of the peptide and is irrelevant to the Cu(II) redox reaction. The peak potential is the same as that of Aβ(1−42) reported by and attributed to the Tyr-10 residue by Vestergaard et al. (*50*). That the voltammogram of tyrosine solution alone (inset in Figure 3) also showed an oxidation peak at a similar potential confirms our assignment. A tyrosine residue could undergo a two-electron, two-proton oxidation reaction (*51*):

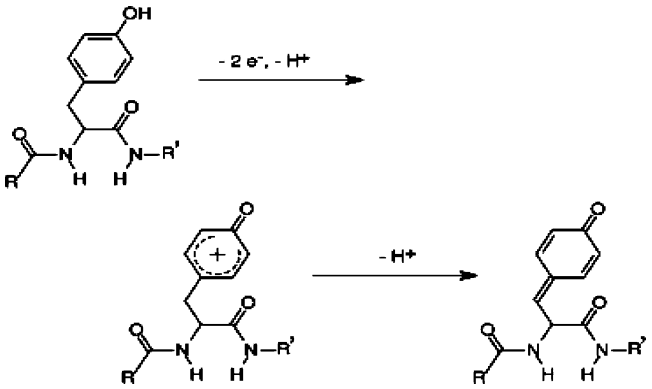

In view that the hydrophobic segment in the Aβ−Cu(II) complex may affect the Aβ redox behavior, we conducted voltammetric experiments on Aβ(1−28) in the absence and presence of Cu(II). Superimposed in Figure 4 are the voltammograms of Aβ(1−28) alone (dashed curve) and Aβ(1−28) in the presence of an equimolar amount of Cu(II) (solid curve). The remarkable resemblance in the peak shapes between Aβ(1−16)−Cu(II) and Aβ(1−28)−Cu(II) indicates that the more hydrophobic segment in Aβ(1−28) does not affect the redox potentials of both the Cu(II) center and the Tyr-10 residue. In addition, Aβ(1−28) (dashed curve) has similar redox behavior as Aβ(1−16). The main difference is that Aβ(1−28) is more prone to aggregation and causes a more significant adsorption onto the electrode surface. To alleviate this effect, we decreased the concentration of Aβ(1−28) for the acquisition of the voltammograms in Figure 4. Again, analogous to Aβ(1−16), Aβ(1−28) displayed an oxidation peak at ca. 0.78 V, which can be ascribed to the Tyr-10 oxidation.

To clearly illustrate the effect of O_2 on the magnitude of the Aβ−Cu(II) reduction peak, we subtracted the voltammograms of Aβ(1−28)−Cu(II) in a N_2-purged solution from those of the same solution saturated with air (Figure 5). The plateaus at slow scan rates (e.g., 0.02 V/s) developed into peaks at higher scan rates. These features are again typical of an electrocatalytic reduction (*49*) and are also consistent with our findings related to Aβ(1−16) (vide supra). For oxygen to be catalytically reduced, oxygen molecules need to diffuse to and become associated with the newly electrogenerated Aβ(1−28)−Cu(I) center. We should note that, without background subtraction, the dependence of the steady-state current on O_2 purged into the solution is not as obvious. This suggests that the O_2 reduction is a diffusion-controlled process. Thus, O_2, which is hydrophobic, appears to have interacted more strongly with the hydrophobic segment inherent in Aβ(1−28), and consequently its movement toward the Aβ−Cu(II) center is retarded (*52*).

We then extended the same approach to the study of Aβ(1−42) and its complex with Cu(II). Since Aβ(1−42) has the strongest propensity to form aggregates, we added a small amount of dimethyl sulfoxide (see Materials and Methods) into the solution to impede the Aβ aggregation and to improve the reproducibility of the experiment. Several points can be extracted from the voltammograms in Figure 6. First, in the cathodic range (solid curve), the redox behavior of the Aβ(1−42)−Cu(II) is highly comparable to those of the Aβ(1−16) and Aβ(1−28) counterparts. Accordingly, we assigned the peak at ~0.02 V to the reduction of Aβ(1−42)−Cu(II) to Aβ(1−42)−Cu(I) and conclude that the redox potential of the Cu(II) center remains largely unaffected by the length of the hydrophobic segment of Aβ. Although the reduction current is much greater than the oxidation current during scan reversal, purging the solution with oxygen and nitrogen led to little change in the peak heights. This is in contrast to the cases of the shorter Aβ variants (cf. Figures 3 and 5). The insensitivity of reduction or oxidation current

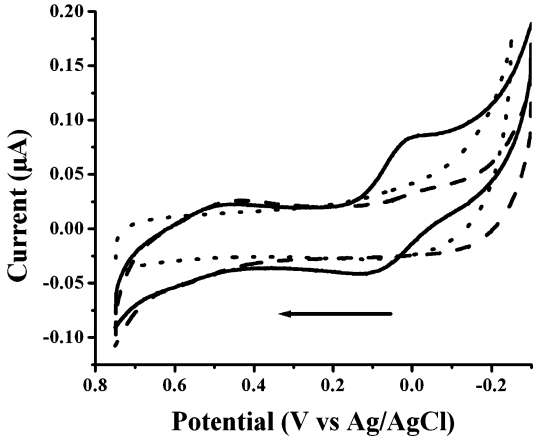

FIGURE 6: Cyclic voltammograms of 50 μM Aβ(1−42) (dashed curve) and a mixture of 50 μM Aβ(1−42) and 50 μM Cu(II) (solid curve) in a 5 mM phosphate buffer containing 0.1 M Na_2SO_4 and 10% dimethyl sulfoxide (pH 7.4). The background voltammogram was collected from the same electrolyte solution without Aβ(1−42) and Cu(II) (dotted curve). A glassy carbon disk electrode with a diameter of 3 mm was used as the working electrode. The scan rate was 20 mV/s.

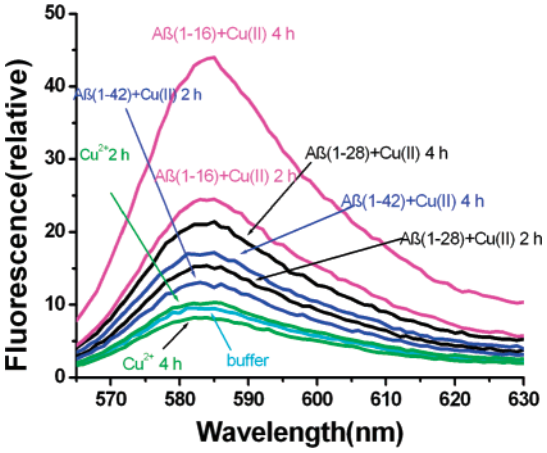

FIGURE 7: Fluorescence spectra of resorufin for mixtures containing Cu(II) and different Aβ species upon electrolyses for different times: 100 μM Aβ(1−16)−Cu(II) (pink curves), 100 μM Aβ(1−28)−Cu(II) (black curves), 50 μM Aβ(1−42)−Cu(II) (blue curves), 100 μM Cu(II) solution (green curves), and buffer solution (light blue curve). In the electrolyses, a normal three-electrode system was used, and a glassy carbon working electrode with an area of 0.071 cm^2 was held at 0.07 V. The solution volume for each was 300 μL. The electrolysis times are indicated next to the respective curves.

of the Aβ(1−42)−Cu(II) complex to the oxygen concentration could be caused by the slow coordination of oxygen molecules with the Aβ(1−42)−Cu(I) center due to the greater steric hindrance imposed by the longer length and the greater hydrophobicity of the Aβ(1−42) strand.

In the anodic range of the CV, a pair of small peaks, with the reduction peak potential at ca. 0.48 V and the oxidation peak potential at ca. 0.6 V, were observed. Again, these peaks are independent of Cu(II), since the peaks in solid and dashed curves in Figure 6 are almost congruent in this range. These peaks were assigned to the redox reaction of the Cu(II) center to its Cu(I) counterpart by Huang et al. (*35*). However, given its close proximity to the oxidation peak of Tyr-10 [cf. inset of Figure 3 and the reported value (*50*)] and its independence of Cu(II) in the solution, we feel that the assignment to the Tyr-10 redox reaction is more plausible. The greater reversibility of tyrosine oxidation in Aβ(1−42) with respect to those of Aβ(1−16) and Aβ(1−28) may be partially contributed by the adsorbate nature of Aβ(1−42). Moreover, it is well-known that adsorption of redox species onto the electrode tends to yield redox peaks whose positions are different than those originated from the soluble species (*49*).

The Aβ−Cu(I) Complex Catalyzes the Reduction of Oxygen to Hydrogen Peroxide. As mentioned above, the reduced form of the Aβ−Cu(II) complex can catalyze oxygen reduction, producing H_2O_2 as one of the possible products (*30*, *35*, *37*). To directly link the redox state of the Cu-containing Aβ complex to the H_2O_2 production, we carried out spectrofluorometric detection of H_2O_2 from Aβ-(1−16)−Cu(II), Aβ(1−28)−Cu(II), and Aβ(1−42)−Cu(II) solutions that had been subject to controlled potential electrolyses.

After electrolyses of these solutions at 0.07 V for a period of time, the solutions were analyzed by a hydrogen peroxide detection kit. We chose 0.07 V because it is at the plateaus of the electrocatalytic reduction peaks of all the Aβ variants (thin solid curve in Figure 3 and solid curves in Figures 4 and 6). At this potential the complication of possible catalytic reduction of oxygen by unbound copper ion can also be excluded [i.e., the potential is more positive than the onset potential of free Cu(II) reduction; cf. the dashed curve in Figure 3]. As shown in Figure 7, for all three Aβ variants, the fluorescence peak heights increase with the electrolysis time. Moreover, the resorufin fluorescence peaks are significantly greater than those in the buffer and Cu(II) solutions. Notice that the fluorescence intensity from the electrolyzed Cu(II) solution was not different than that from the buffer solution, again suggesting that the catalytic reaction involving Cu(II) and O_2 occurs at a different potential. Aβ−Cu(II) complex solutions without being electrolyzed also exhibited similar responses to those of the buffer solution. All of these observations indicate that it is the reduced Aβ−Cu(II) complex that is responsible for the H_2O_2 production.

A point particularly worth noting is that the fluorescence intensity increases inversely with the length of the Aβ variants. This explains why the catalytic reduction current becomes less sensitive to the concentration of dissolved oxygen as the Aβ strand becomes longer. Such a consistency reinforces our earlier contention that the movement of oxygen to the electrogenerated Cu(I) center is dependent on both the length and hydrophobicity of the Aβ strand.

DISCUSSION

As mentioned in the introduction, it is generally believed that the Cu(II) binding domain in Aβ is within the segment comprising residues 1−14 (*30*, *34*, *38*, *53*), with His-6, His-13, and His-14 having the strongest metal binding affinities. Our ESI-FTICR-MS study has demonstrated that the binding ratio between Cu(II) and Aβ(1−28) or Aβ(1−42) is 1:1, which is consistent with results by Karr et al. (*38*) and Garzon-Rodriguez et al. (*54*). We did not find other binding ratios as reported by others (*29*, *34*). The ESI-FTICR-MS results are also in good agreement with our voltammetric data, which showed that the reduction current of the Aβ-(1−16)−Cu(II) complex leveled off once the molar ratio between Cu(II) and Aβ(1−16) had exceeded 1:1.

The reduction potentials of Aβ−Cu(II) deduced from Figures 3, 4, and 6 allowed us to gain insight about the

Table 3: Redox Potentials of the Aβ−Cu(II) Complex and Common Redox Species of Biological Relevance

system	$E^{0'}$(V vs NHE)	ref
norepinephrine	0.384	*90*
epinephrine	0.372	*90*
dopamine	0.370	*91*
O_2/H_2O_2	0.295	*93*
cytochrome *a*	0.290	*90*
Aβ−Cu(II)	0.280	
cytochrome *c*	0.250	*90*
hemoglobin	0.152	*92*
$CoQ/CoQH_2$ [a]	0.100	*90*
ascorbic acid	0.051	*92*
cytochrome *b*	0.040	*90*
fumarate/succinate	0.031	*93*
myoglobin	0.005	*90*
crotonyl-CoA/butyryl-CoA	−0.015	*93*
$FMN/FMNH_2$ [b]	−0.120	*90*
oxaloacetate/malate	−0.166	*93*
pyruvate/lactate	−0.185	*93*
glutathione	−0.228	*90*
vitamin B_{12}	−0.244	*90*
$NAD^+/NADH$ [c]	−0.320	*90*
$FAD/FADH_2$ [d]	−0.327	*90*

[a] Coenzyme Q (ubiquinone) oxidized/reduced forms. [b] Flavin mononucleotide oxidized/reduced forms. [c] Nicotinamide adenine dinucleotide oxidized/reduced forms. [d] Flavin adenine dinucleotide oxidized/reduced forms.

factors or redox species that could be involved in the reduction of the Aβ−Cu(II) complex in the cellular milieu. Thus, for example, to reduce Aβ(1−42)−Cu(II), a species must have a reduction potential that is more negative (cathodic) than 0.08 V vs Ag/AgCl or 0.28 V vs normal hydrogen electrode, NHE (cf. Figure 6 and Table 3). Since the Tyr-10 redox peak appeared at ∼0.78 V, we conclude that Tyr-10 cannot reduce Aβ(1−42)−Cu(II) in vitro. Several reports have suggested that Tyr-10 participates in the metal ion coordination. A Raman analysis of samples from deceased AD patients' brains indicated that the tyrosine residue in Aβ(1−42) was oxidized (*28*). Thus, it is clear that the Aβ−Cu(II) complex is not the sole species responsible for the Tyr-10 oxidation, and other cellular species or processes must be involved. Another amino acid residue that is susceptible to oxidation and has been implicated in the reduction of Aβ−Cu(II) and generation of ROS such as H_2O_2 is Met-35 (*30*, *45*, *55*). However, from the ESI-FTICR-MS data, we did not find ions corresponding to oxidized or chemically modified (e.g., oxygenated adducts) Aβ(1−42) and/or Aβ(1−42)−Cu(II). Previously, the peak potential for the Met-35 oxidation to its radical cation has been reported to exceed 1.3 V vs Ag/AgCl in aqueous solution (*56*). Such a value is almost 1.2 V more *positive* than the Aβ−Cu(II) reduction potential, suggesting that Met-35 would not be a viable reductant under the in vitro condition. Moreover, in the natively unstructured Aβ(1−40) or Aβ(1−42) monomer, there is a wide separation between the metal center (close to the N terminus) and Met-35 (in the vicinity of the C terminus), which is unfavorable for facile ET. Therefore, on the basis of the MS and voltammetric data, we also ruled out the possibility that Met-35 had undergone oxidation reactions with Cu(II) in solution and/or Cu(II) in the complex without involving other cellular species. This conclusion is in agreement with what was found by Hou and Zagorski (*39*).

In solution, Aβ binds Cu(II), and under an externally applied potential, the resultant Aβ−Cu(II) complex can be reduced to Aβ−Cu(I), once the cathodic scan has passed ∼0.080 V:

$$A\beta\text{−Cu(II)} + e^- = A\beta\text{−Cu(I)} \quad (1)$$

Notice that the reduction potential for the Aβ−Cu(II) complex is quite different than that reported by Huang et al. (*35*) As the redox potentials of copper complexed by histidine-containing peptides are in the range between −0.1 and 0.1 V (*46*−*48*, *57*, *58*), we believe that the redox potential around 0.1 V is more reasonable.

In the presence of dissolved oxygen, the electroreduced Aβ−Cu(I) center could react with O_2 in solution, producing H_2O_2:

$$2A\beta\text{−Cu(I)} + O_2 + 2H^+ = 2A\beta\text{−Cu(II)} + H_2O_2 \quad (2)$$

The above reaction is responsible for the O_2-dependent reduction peaks exhibited in Figures 3−6. As the potential for the Aβ−Cu(II)/Aβ−Cu(I) (0.28 V vs NHE) is lower than that for O_2/H_2O_2 (0.295 V vs NHE, Table 3), reaction 2 is thermodynamically allowed. A much higher potential for Aβ−Cu(II)/Aβ−Cu(I), as that reported in ref (*35*) (0.55 V vs Ag/AgCl), however, would cause reaction 2 to proceed in the reverse direction (i.e., H_2O_2 oxidation). Thus, our measured potential value explains the catalytic reduction of O_2 to H_2O_2 better. We should point out that the present study cannot rule out the possibility that some O_2 might be reduced to H_2O in a similar fashion to that catalyzed by Cu(II)-containing enzymes such as laccase (*59*). However, the Aβ−Cu(II) complexes are not considered to be "enzymes", and the direct four-electron reduction of O_2 to H_2O typically involves multiple copper centers (*59*). Furthermore, based on the H_2O_2 detected and other published data (*37*), the reactions outlined above should constitute the major mechanism. To further confirm the proposed mechanism, we simulated the kinetics of ET reaction and the follow-up catalytic oxygen reduction. The simulated voltammogram, overlaid with the experimentally measured one, is provided in the Supporting Information, together with the parameters used for the simulation. The heterogeneous ET rate constant for Aβ(1−16)−Cu(II) at the electrode was estimated to be about 5×10^{-4} s^{-1}, and the follow-up catalytic reaction rate constant was deduced to be about 1000 M^{-1} s^{-1}. The reasonable agreement between the experimental and simulated voltmmograms suggests that the proposed mechanism is quite likely. Moreover, the rather high reaction rate constant deduced for eq 2 indicates that there is a strong tendency for the reduced Aβ−Cu(II) complex to catalytically reduce O_2 to H_2O_2. The rapid depletion of ascorbic acid (Figure S6), initiated by the Aβ−Cu(II) complex, indicates the fast turnover rate (vide infra).

On the basis of our spectrofluorometric measurements (Figure 7), it is clear that a prerequisite for H_2O_2 generation is the conversion of Aβ−Cu(II) to Aβ−Cu(I). The difference in the dependence of the catalytic peak currents on the O_2 content in solution among the three Aβ−Cu(II) complexes implies that, in AD patients, the amount of H_2O_2 produced in reaction 2 is likely to be dependent on the Aβ sequence and length. It is generally known that Aβ(1−42) has a much

stronger tendency to aggregate than Aβ(1−40), and the Aβ-(1−42) content in senile plaques of AD patients is disproportionately high (*60*). Given the relatively high affinity of Aβ species toward metal ions, it has been shown that Aβ and its aggregates, upon complexation with redox-active metal ions such as Cu(II) and Fe(III), can generate H_2O_2 (*35*, *37*). The level of H_2O_2 can be sufficiently high to cause cell death (*37*). On the basis of the aforementioned dependence of H_2O_2 amount on the strand length of Aβ species, we postulate that there might exist an alternative process responsible for the slow onset of AD symptom. If reactions 1 and 2 are at work, the amount of H_2O_2 generated must be dependent on all of the reactants [i.e., Aβ, Cu(II), and O_2]. Since in senile plaques the content of Aβ and concentration of Cu(II) are high and the function of brains requires a constant supply of large amounts of O_2 (*61*), one would expect that H_2O_2 concentration would be substantially high. In addition to metabolic degradation of species that can potentially generate ROS and scavenging of ROS (including H_2O_2) by antioxidants, we think that the slow diffusion of O_2 to the metal center in the Cu(II)−Aβ complex should have dramatically hindered the H_2O_2 generation. Regarding the dependence of H_2O_2 generation on the Aβ sequence, it is interesting to note that mice do not develop AD (*62*), and its Aβ is mutated at two of the metal binding sites, viz., His-13 and Tyr-10 (replaced by Arg and Phe, respectively). The decreased binding affinity of such a mutated Aβ toward Cu(II) leads to a dramatically lower H_2O_2 production (*37*). In the case of familial AD, the Aβ is point-mutated, which causes early onset AD. Interestingly, none of the mutations occurs in the metal binding region. These facts strongly suggest the important roles of metal binding and H_2O_2 production in the pathogenesis of AD.

During the CV scan reversal, Aβ−Cu(I) molecules that have not been completely oxidized by O_2 in solution (cf. thin solid curve in Figure 3 and thick solid curves in Figures 4 and 6), will be reoxidized:

$$A\beta\text{−Cu(I)} - e^- = A\beta\text{−Cu(II)} \quad (3)$$

The concentration of Aβ−Cu(I) depends on the catalytic turnover rate, which is in turn governed by the accessibility of the Aβ−Cu(I) complex to oxygen and the oxygen concentration in solution. A declined oxygen level in solution results in the availability of more Aβ−Cu(I), which leads to a greater oxidation current during the reverse potential scan (cf. Figure 3). The function of metalloproteins in a biological process involving O_2 requires the binding to and activation of diatomic O_2 molecules by the metal center(s). Recent studies have captured the O_2-containing intermediates (*63*, *64*). Similarly, the catalytic reduction of O_2 by Aβ−Cu(I) also entails the binding of O_2 to the copper center. It is conceivable that a longer Aβ segment will increase the steric hindrance for O_2 binding to the copper center and decrease the catalytic turnover rate. This is in accord with our experimental results. Given the slow and gradual development of AD, our contention appears to be plausible.

As stated in previous sections, a prerequisite for the catalytic production of H_2O_2 is the reduction of Aβ−Cu(II) to Aβ−Cu(I) and the subsequent binding of O_2. This process would not occur in vitro without a suitable electron donor. However, the Aβ−Cu(II) complex could be reduced in vivo by redox reactions involving easily oxidizable cellular species (i.e., antioxidants). There exists a wide range of intracellular and extracellular electroactive species and antioxidants, some of which, together with their reduction potentials, are listed in Table 3.

Species whose reduction potentials are more positive than the Aβ−Cu(II) reduction potential (0.280 V) are incapable of reducing Aβ−Cu(II). These include some important redox-active neurotransmitters such as dopamine, epinephrine, and norepinephrine. This is interesting, since, to our knowledge, there is no evidence directly linking the appearance of Aβ aggregates or senile plaques to the deficiency of these neurotransmitters. It is a well-known fact that another neurodegenerative disease, Parkinson's disease, is directly related to dopamine deficiency and loss of dopaminogenic neurons. The species listed in Table 3 that could (i.e., potentials more negative) reduce the Aβ−Cu(II) complex can be classified into three categories: extracelluar species (e.g., ascorbic acid), intracellular redox buffers (e.g., glutathione), and membrane-bound redox species (especially those associated with mitochondria that govern cellular respiratory processes and bioenergetics).

Outside the neuronal cells, reduction of Aβ−Cu(II) to Aβ−Cu(I) by ascorbic acid and vitamin B_{12} is thermodynamically favored (Table 3). The reduced Aβ−Cu(I) can then catalyze the reduction of oxygen to form hydrogen peroxide. The as-formed hydrogen peroxide can either react further with antioxidants such as ascorbic acid and vitamin B_{12} or attack cell membrane and other organelles in brain. This certainly will deplete the antioxidants and damage the cellular defense system, making the cells vulnerable. To verify that the Aβ−Cu(II) reduction by ascorbic acid is kinetically facile, we acquired CVs of ascorbic acid in the absence and presence of Aβ−Cu(II). As shown in Figure S6, without Aβ-(1−16) and Cu(II) in the solution, an irreversible oxidation peak of ascorbic acid at ca. 0.42 V was observed. The irreversible reduction is due to the ring-closure reaction following the ET reaction, as shown in eq 4:

$$\text{ascorbic acid} + H_2O = \text{dehydroascorbic acid} + 2H^+ + 2e^- \quad (4)$$

When Aβ−Cu(II) is present, the addition of an equimolar amount of ascorbic acid did not show the characteristic irreversible ascorbic acid oxidation peak. Only after the addition a few more molar equivalents did the oxidation peak appear in the first potential scan (Figure S6). Interestingly, the peak quickly disappeared in the second scan. When the solution was thoroughly purged, the ascorbic acid oxidation peak was observable regardless of the presence of Aβ−Cu(II). These observations thus demonstrate that ascorbic acid can rapidly reduce Aβ−Cu(II) to Aβ−Cu(I) and the resultant Aβ−Cu(I) catalyzes the oxygen reduction. The overall catalytic redox reaction cycle converts ascorbic acid to dehydroacorbic acid. The rapid depletion of ascorbic acid is also consistent with the high chemical reaction rate constant in the aforementioned kinetic simulation.

There have been many mechanisms suggesting that Aβ penetrates cell membranes and enters cytoplasma (*65*−*67*). Aβ has been shown to exist inside (*22*, *68*−*70*) and outside of neuronal cells in AD-affected brains. In PC12 cells and human fibroblasts Aβ oligomers were found to adsorb onto

the cell surface and became internalized into the cytosol (*71*, *72*). Given the relatively high binding affinity of Aβ to Cu(II) (*29*), Cu(II)-bound Aβ monomers and oligomers should be capable of penetrating the neuronal cell membrane. In addition, it is purported that APP from which Aβ is cleaved can function as a copper chaperone, regulating the intracellular copper concentration and homeostasis (*73*). Inside the neuronal cells, the glutathione redox couple (GSH/GSSG), present at millimolar concentrations, has a high redox buffering capacity. The GSH/GSSG couple not only maintains the function of mitochondria (*74*) but also regulates the apoptosis of cells (*75*−*79*). From Table 3, the reduction of the Aβ−Cu(II) complex to Aβ−Cu(I) by glutathione is favored thermodynamically, and H_2O_2 produced via reaction 2 could consequently disrupt the potentiation of the GSH/GSSG couple. The possible decline in the cellular glutathione may not only induce abnormal apoptosis but also cause dysfunction of mitochondria. Another intracellular species whose reduction potential is lower than the Aβ−Cu(II) complex is pyruvate, which serves as the fuel for the mitochondria-mediated metabolic process. As shown by the potential values in Table 3, a redox reaction between Aβ−Cu(II) and pyruvate is possible. Similarly, given the presence of a high concentration of O_2 in brain and particularly in neuronal cells (*61*), the catalytic reduction of O_2 to H_2O_2 by Aβ−Cu(I) is likely to occur. The H_2O_2 would subsequently oxidize more pyruvate molecules and cause a depletion of the cellular pyruvate concentration. As a result, ATP production is decreased and mitochondria are starved energetically. This process may have some relevance to the observed decline in the production of ATP in AD patients (*80*−*83*). In line with our suggestion, therapeutic treatments of AD patients with pyruvate derivatives have shown promise in alleviating AD symptoms (*84*).

It has been well documented that mitochondrial insufficiencies contribute significantly to the pathophysiology of AD and mitochondrial dysfunction is also a hallmark of AD (*80*, *85*−*87*). However, the intricate relationship between AD and mitochondrial dysfunction awaits further elucidation. Aβ has been found to exist inside mitochondria and deposited on mitochondria membranes in AD brains (*81*, *88*). Recent studies demonstrated that, in the presence of Cu(II), Aβ inhibits the activity of cytochrome *c* oxidase in mitochondria (*22*−*24*, *82*). This provides a possible link between the dysfunction of mitochondria and Aβ−Cu(II). The function of mitochondria relies on the uninterrupted ET processes in the cascade of events at the membrane and in the intermembrane space. As shown in Table 3, the redox reactions of Aβ−Cu(II) with nicotinamide adenine dinucleotide (NADH), flavin mononucleotide ($FMNH_2$), flavin adenine dinucleotide ($FADH_2$), coenzyme Q ($CoQH_2$), cytochrome *b*, cytochrome c_1, and cytochrome *c* in the ET chain are all thermodynamically allowed. If there is a reaction of Aβ−Cu(II) with any of the species, the normal electron flow will be sidetracked, leading to dysfunction of mitochondria and triggering a mitochondrial death pathway. We should note that mitochondrial dysfunction has been shown to be associated with the AD development (*80*, *85*, *86*, *89*).

Overall, the Aβ−Cu(II) complex can react with redox-active molecules essential to neuronal cells and present in biological fluids. Thus, the accurate measurements of the redox potentials of various Aβ−Cu(II) species and the confirmation of H_2O_2 generation by the Aβ−Cu(I) complex provides new insight into AD pathogenesis and offers some possible interpretations about certain AD symptoms and the roles of metal ions in AD neuropathology.

CONCLUSIONS

We have studied, for the first time, the interaction of Aβ with Cu(II) by high-resolution mass spectrometry. It reveals that Cu(II) coordinates with Aβ in a 1:1 ratio. Independent of the methionine residue, the oxidation state of the copper center in the complex is 2+. The presumed reduction reaction of the Cu(II) center to Cu(I) cannot occur in vitro. The redox chemistry of the complexes of Aβ(1−16), Aβ(1−28), or Aβ(1−42) with Cu(II) was systematically investigated by cyclic voltammetry, and the redox potential for the reduction of the copper center was determined to be 0.08 V (vs Ag/AgCl). The Aβ−Cu(I) electrogenerated was found to catalyze the reduction of oxygen and produce hydrogen peroxide. The remarkable similarity among the voltammetric behaviors of these three complexes excludes the possibility that methionine-35 can be oxidized by the Cu(II) center. In addition, we found that the diffusion of oxygen to the Cu(II) center is dependent on the peptide length (steric hindrance) and hydrophobicity. To our knowledge, this is the first work showing that Aβ−Cu(I) can be controllably generated and studied in the presence and absence of O_2. The implication of the redox properties of the complex is discussed in the biological context. On the basis of the redox potentials of Aβ, Aβ−Cu(II) complexes, and common redox-active biomolecules, a number of redox reactions could occur. As a result, antioxidants may be depleted, which may destroy the normal protective system against oxidative stress. Using voltammetry and digital simulation, we show that the thermodynamically allowed reduction of Cu(II)−Aβ(1−42) by ascorbic acid is kinetically facile. The redox reactions of the Aβ−Cu(II) complex with species in the ET chain of mitochondria are also thermodynamically favorable. Although whether these reactions occur in vivo remain to be investigated, the possibility raises an important aspect that such reactions could sidetrack the normal electron flow in the respiratory process of mitochondria.

SUPPORTING INFORMATION AVAILABLE

ESI-FTICR mass spectra of Aβ(1−28) and Aβ(1−42), a linear ion trap mass spectrum of the Aβ(1−42)−Cu(II) complex, a voltammogram of Cu(II) in a thoroughly deaerated solution, voltammograms of ascorbic acid in the presence of Aβ(1−16)−Cu(II), and a table showing the relation between the reduction peak current of the Aβ(1−16)−Cu(II) complex and the molar ratio of Cu(II) and Aβ(1−16). This material is available free of charge via the Internet at http://pubs.acs.org.

REFERENCES

1. Kang, J., Lemaire, H. G., Unterbeck, A., Salbaum, J. M., Masters, C. L., Grzeschik, K. H., Multihaup, G., Beyreuther, K., and Muller-Hill, B. (1987) Amyloid production secretase, *Nature 325*, 733−736.
2. Masters, C. L., Simms, G., Weinman, N. A., Multhaup, G., McDonald, B. L., and Beyreuther, K. (1985) Amyloid plaque core protein in Alzheimer disease and down syndrome, *Proc. Natl. Acad. Sci. U.S.A. 82*, 4245−4249.

3. Glenner, G. C., and Wong, C. W. (1984) Alzheimer's disease: initial report of the purification and charaterization of a novel cerebrovascular amyloid protein, *Biochem. Biophys. Res. Commun. 120*, 885−890.
4. Hardy, J. A., and Higgins, G. A. (1992) Alzheimer's disease: the amyloid cascade hypothesis, *Science 256*, 184−185.
5. Hensley, K., Hall, N., Subramaniam, R., Cole, P., Harris, M., Aksenov, M., Aksenova, M., Gabbita, P., Wu, J. F., Carney, J. M., Lovell, M., Markesbery, W. R., and Butterfield, D. A. (1995) Brain regional correspondence between Alzheimer's disease histopathology and biomarkers of protein oxidation, *J. Neurochem. 65*, 2146−2156.
6. Smith, C. D., Carney, J. M., Starke-Reed, P. E., Oliver, C. N., Stadtman, E. R., Floyd, R. A., and Markesbery, W. R. (1991) Excess brain oxidation and enzyme dysfunction in normal aging and Alzheimer's disease, *Proc. Natl. Acad. Sci. U.S.A. 88*, 10540−10543.
7. Lyras, L., Cains, N. J., Jenner, A., Jenner, P., and Halliwell, B. (1997) An assessment of oxidative damage to proteins, lipids and DNA in brains from patients with alzheimer's disease, *J. Neurochem. 68*, 2061−2069.
8. Markesbery, W. R., and Carney, J. M. (1999) Oxidative alterations in Alzheimer's disease, *Brain Pathol. 9*, 133−146.
9. Mecocci, P., MacGarvey, U., Kaufman, A. E., Koontz, D., Shoffner, J. M., Wallace, D. C., and Beal, M. F. (1993) Oxidative damage to mitochondrial DNA show marked age-dependent increases in human brain, *Ann. Neurol. 34*, 609−616.
10. Mecocci, P., MacGarvey, U., and Beal, M. F. (1994) Oxidative damage to mitochodrial DNA is increased in Alzheimer's disease, *Ann. Neurol. 36*, 747−751.
11. Nitsch, R. M., Bluztajn, J. K., Pittas, A. G., Slack, B. E., Growdon, J. H., and Wurtman, R. J. (1992) Evidence for a membrane defect in Alzheimer's disease brain, *Proc. Natl. Acad. Sci. U.S.A. 89*, 1671−1675.
12. Svennerholm, L., and Gottfries, C. G. (1994) Membrane lipids, selectively diminished in Alzheimer's brains, suggest synapse loss as a primary event in early-onset and demyelination in late-onset form, *J. Neurochem. 62*, 1039−1047.
13. Subbarao, K. V., Richardson, J. S., and Ang, L. C. (1990) Autopsy samples of Alzheimer's cortex show increased peroxidation *in vitro*, *J. Neurochem. 55*, 342−345.
14. Marcus, D. L., Thomas, C., Rodriguez, C., Simberkoff, K., Tsai, J. S., Strafaci, J. A., and Freedman, M. L. (1998) Increased peroxidation and reduced antioxidant enzyme activity in Alzheimer's disease, *Exp. Neurol. 150*, 40−44.
15. Varadarajan, S., Yatin, S., Aksenova, M., and Butterfield, D. A. (2000) Alzheimer's amyloid beta-peptide-associated free radical oxidative stress and neurotoxicity, *J. Struct. Biol. 130*, 184−208.
16. Sims, N. R. (1996) Energy metabolism, oxidative stress and neuronal degeneration in Alzheimer's disease, *Neurodegeneration 5*, 435−440.
17. Beal, M. F. (1998) Mitochondrial dysfunction in neurodegenerative diseases, *Biochim. Biophys. Acta 1366*, 211−223.
18. Parker, W. D., Jr. (1991) Cytochrome *c* oxidase deficiency in Alzheimer's disease, *Ann. N.Y. Acad. Sci. 640*, 59−64.
19. de La Monte, S. M., Luong, T., Neely, T. R., Robinson, D., and Wands, J. R. (2000) Mitochondrial DNA damage as a mechanism of cell loss in Alzheimer's disease, *Lab. Invest. 80*, 1323−1335.
20. Maurer, I., Zierz, S., and Moller, H. J. (2000) A selective defect of cytochrome *c* oxidase is present in brain of Alzheimer's disease patients, *Neuobiol. Aging 21*, 455−462.
21. Valla, J., Bernt, J. D., and Gonzalez-Lima, F. (2001) Energy hypo metabolism in poterior cingulate cortex of Alzheimer's patients: superficial laminar cytochrome oxidase associated with disease duration, *J. Neurosci. 21*, 4923−4930.
22. Deshpande, A., Mina, E., Glabe, C., and Busciglio, J. (2006) Different conformations of amyloid beta induce neurotoxicity by distinct mechanisms in human cortical neurons, *J. Neurosci. 26*, 6011−6018.
23. Crouch, P. J., Barnham, K. J., Duce, J. A., Blake, R. E., Masters, C. L., and Trounce, I. A. (2006) Copper-dependent inhibition of cytochrome *c* oxidase by abeta requires reduced methionine at residue 35 of the abeta peptide, *J. Neurochem. 99*, 226−236.
24. Crouch, P. J., Blake, R., Duce, J. A., Ciccotosto, G. D., Li, Q.-X., Barnham, K. J., Curtain, C. C., Cherny, R. A., Cappai, R., Dyrks, T., Masters, C. L., and Trounce, I. A. (2005) Copper-dependent inhibition of human cytochrome *c* oxidase by a dimeric conformer of amyloid-beta, *J. Neurosci. 19*, 672−679.
25. Schlief, M. L., Craig, A. M., and Gitlin, J. D. (2005) NMDA receptor activation mediates copper homeostasis in hippocampal neurons, *J. Neurosci. 25*, 239−246.
26. Howell, G. A., Welch, M. G., and Frederickson, C. J. (1984) Stimulation-induced uptake and release of zinc in hippocampal slices, *Nature 308*, 736−738.
27. Curtain, C. C., Ali, F. E., Smith, D. G., Bush, A. I., Masters, C. L., and Barnham, K. J. (2003) Metal ions, pH, and cholesterol regulate the interactions of Alzheimer's disease amyloid-β peptide with membrane lipid, *J. Biol. Chem. 278*, 2977−2982.
28. Dong, J., Atwood, C. S., Anderson, V. E., Siedlak, S. L., Smith, M. A., Perry, G., and Carey, P. R. (2003) Metal binding and oxidation of amyloid-β within isolated senile plaque cores: Raman microscopic evidence, *Biochemistry 42*, 2768−2773.
29. Atwood, C. S., Scarpa, R. C., Huang, X., Moir, R. D., Jones, W. D., Fairlie, D. P., Tanzi, R. E., and Bush, A. I. (2000) Characterization of copper interactions with Alzheimer amyloid-β peptides: identification of an attomolar-affinity copper binding site on amyloid β_{1-42}, *J. Neurochem. 75*, 1219−1233.
30. Curtain, C. C., Ali, F., Volitakisi, I., Chernyi, R. A., Norton, R. S., Beyreuther, K., Barrow, C. J., Mastersi, C. L., Bush, A. I., and Barnham, K. J. (2001) Alzheimer's disease amyloid-β binds copper and zinc to generate an allosterically ordered membrane-penetrating structure containing superoxide dismutase-like subunits, *J. Biol. Chem. 276*, 20466−20473.
31. Kowalik-Jankowska, T., Ruta, M., Wisniewska, K., and Lankiewicz, L. (2003) Coordination abilities of the 1−16 and 1−28 fragments of β-amyloid peptide towards copper(II) ions: a combined potentiometric and spectroscopic study, *J. Inorg. Biochem. 95*, 270−282.
32. Lovell, M. A., Robertson, J. D., Teesdale, W. J., Campbell, J. L., and Mardesbery, W. R. (1998) Copper, iron and zinc in Alzheimer's disease senile plaques, *J. Neurol. Sci. 158*, 47−52.
33. Nishino, S., and Nishida, Y. (2001) Oxygenation of amyloid beta-peptide (1−40) by copper(II) complex and hydrogen peroxide system, *Inorg. Chem. Commun. 4*, 86−89.
34. Syme, C. D., Nadal, R. C., Rigby, S. E. J., and Viles, J. H. (2004) Copper binding to the amyloid-beta peptide associated with Alzheimer's disease, *J. Biol. Chem. 279*, 18169−18177.
35. Huang, X., Cuajungco, M. P., Atwood, C. S., Hartshorn, M. A., Tyntall, J. D. A., Hanson, G. R., Stokes, K. C., Leopold, M., Multhaup, G., Goldstein, L. E., Scarpa, R. C., Saunders, A. J., Lim, J., Moir, R. D., Glabe, C., Bowden, E. F., Masters, C. L., Fairlie, D. P., Tanzi, R. E., and Bush, A. (1999) Cu(II) potentiation of Alzheimer's Aβ neurotoxicity, *J. Biol. Chem. 274*, 37111−37116.
36. Lynch, T., Cherny, R. A., and Bush, A. I. (2000) Oxidative processes in Alzheimer's disease: the role of Aβ-metal interactions, *Exp. Gerontol. 35*, 445−451.
37. Opazo, C., Huang, X., Cherny, R. A., Moir, R. D., Roher, A. E., White, A. R., Cappai, R., Masters, C. L., Tanzi, R. E., Inetstrosa, N. C., and Bush, A. I. (2002) Metalloenzyme-like activity of Alzheimer's disease beta-amyloid, *J. Biol. Chem. 277*, 40302−40308.
38. Karr, J. W., Kaupp, L. J., and Szalai, V. A. (2004) Amyloid-β binds Cu^{2+} in a mononuclear metal ion binding site, *J. Am. Chem. Soc. 126*, 13534−13538.
39. Hou, L., and Zagorski, M. G. (2006) NMR reveals anomalous copper(II) binding to the amyloid Aβ peptide of Alzheimer's disease, *J. Am. Chem. Soc. 128*, 9260−9261.
40. Atwood, C. S., Moir, R. D., Huang, X., Scarpa, R. C., Bacarra, N. M. E., Romano, D. M., Hartshorn, M. A., Tanzi, R. E., and Bush, A. I. (1998) Dramatic aggregation of Alzheimer Aβ by Cu(II) is induced by conditions representing physiological acidosis, *J. Biol. Chem. 273*, 12817−12826.
41. Bott, A. W. (1999) Redox properties of electron transfer metalloproteins, *Curr. Sep. 18*, 47−54.
42. Fezui, Y., Hartley, D., Harper, J., Khurana, R., Walsh, D., Condron, M., Selkoe, D., Lansbury, P., Fink, A. L., and Teplow, D. (2000) An improved meethod of preparing the amyloid β-protein for fibrillogenesis and neurotoxicity experiments, *Amyloid: Int. J. Exp. Clin. Invest. 7*, 166−178.
43. Hou, L., Kang, I., Marchant, R. E., and Zagorski, M. G. (2002) Methionine 35 oxidation reduces fibril assembly of the amyloid Aβ(1−42) peptide of Alzheimer's disease, *J. Biol. Chem. 277*, 40173−40176.
44. Fenn, J. B., Mann, M., Meng, C. K., Wong, S. F., and Whitehouse, C. M. (1989) Electrospray ionization for mass spectrometry of large biomolecules, *Science 246*, 64−71.

45. Schoneich, C., Pogocki, D., Hug, G. L., and Bobrowski, K. (2003) Free radical reactions of methionine in peptides: mechanisms relevant to beta-amyloid oxidation and Alzheimer's disease, *J. Am. Chem. Soc. 125*, 13700−13713.
46. Weng, Y. C., Fan, F.-R. F., and Bard, A. J. (2005) Combinatorial biomimetics. Optimization of a composition of copper(II) poly-L-histidine complex as an electrocatalyst for O_2 reduction by scanning electrochemical microscopy, *J. Am. Chem. Soc. 127*, 17576−17577.
47. Bonomo, R. P., Conte, E., Impellizzeri, G., Pappalardo, G., Purrello, R., and Rizzarelli, E. (1996) Copper(II) complexes with cyclo(L-aspartyl) and cyclo(L-glutamyl-L-glutamyl) derivatives and their antioxidant properties, *J. Chem. Soc., Dalton Trans. 1996*, 3093−3099.
48. Bonomo, R. P., Impellizzeri, G., Pappalardo, G., Purrello, R., Rizzarelli, E., and Tabbi, G. (1998) Coordinating properties of cyclopeptides. Thermodynamic and spectroscopic study on the formation of copper(II) complexes with cyclo(Gly-His)$_4$ and cyclo-(Gly-His-Gly)$_2$ and their superoxide dismutase-like activity, *J. Chem. Soc., Dalton Trans. 1998*, 3851−3857.
49. Bard, A. J., and Faulkner, L. R. (2000) *Electrochemical methods: fundamentals and applications*, 2nd ed., John Wiley & Sons, New York.
50. Vestergaard, M.-D., Kerman, K., Saito, M., Nagatani, N., Takamura, Y., and Tamiya, E. (2005) A rapid label-free electrochemical detection and kinetic study of Alzheimer's amyloid beta aggregation, *J. Am. Chem. Soc. 127*, 11892−11893.
51. Brabec, V., and Mornstein, V. (1980) Electrochemical behavior of proteins at graphite electrodes: II electrooxidation of amino acids, *Biophys. Chem. 12*, 159−165.
52. Halliwell, B., and Gutteridge, J. M. C. (1984) Oxygen toxicity, oxygen radicals, transition metals and disease, *Biochem. J. 219*, 1−14.
53. Miura, T., Suzuki, K., Kohata, N., and Takeuchi, H. (2000) Metal binding modes of Alzheimer's amyloid β-peptide in insoluble aggregates and soluble complexes, *Biochemistry 39*, 7024−7031.
54. Garzon-Rodriguez, W., Yatsimirsky, A. K., and Glabe, C. G. (1999) Binding of Zn(II), Cu(II), and Fe(II) ions to Alzheimer's all peptide studied by fluorescence, *Bioorg. Med. Chem. Lett. 9*, 2243−2248.
55. Varadarajan, S., Kanski, J., Aksenova, M., Lauderback, C., and Butterfield, D. A. (2001) Different mechanisms of oxidative stress and neurotoxicity for Alzheimers Aβ(1−42) and Aβ(25−35), *J. Am. Chem. Soc. 123*, 5625−5631.
56. Sanaullah, Wilson, G. S., and Glass, R. S. (1994) The effect of pH and complexation of amino acid functionality on the redox chemistry of methionine and X-ray structure of [Co(en)$_2$(L-Met)]-$(ClO_4)_2$·H_2O, *J. Inorg. Biochem. 55*, 87−99.
57. Bonomo, R. P., Impellizzeri, G., Pappalardo, G., Rizzarelli, E., and Tabbi, G. (2000) Copper binding modes in the prion octapeptide PHGGGWGQ, a spectroscopic and voltammetric study, *Eur. Chem. J. 6*, 4195−4202.
58. Yang, W., Jarmillo, D., Gooding, J. J., Hibbert, D. B., Zhang, R., Willett, G. D., and Fisher, K. J. (2001) Sub-ppt detection limits for copper ions with Gly-Gly-His modified electrodes, *Chem. Commun. 2001*, 1982−1983.
59. Solomon, E. I., Sundaram, U. M., and Machonkin, T. E. (1996) Multicopper oxidases and oxygenases, *Chem. Rev. 96*, 2563−2605.
60. Morgan, C., Colombres, M., Nunez, M. T., and Inestrosa, N. C. (2004) Structure and function of amyloid in Alzheimer's disease, *Prog. Neurobiol. 74*, 323−349.
61. Kandel, E. R., Schwartz, J. H., and Jessell, T. M. (2000) *Principles of neural science*, McGraw Hill, New York.
62. Vaughan, D. W., and Peters, A. (1981) The structure of neuritic plaque in cerebral cortex of aged rats, *J. Neuropathol. Exp. Neurol. 40*, 472−487.
63. Aboelella, N. W., Reynolds, A. M., and Tolman, W. B. (2004) Catching copper in the act, *Science 304*, 836−837.
64. Prigge, S. T., Eipper, B. A., Mains, R. E., and Amzel, L. M. (2004) Dioxygen binds end-on to mononuclear copper in a precatalytic enzyme complex, *Science 304*, 864−867.
65. Kayed, R., Sokolov, Y., Edmonds, B., McIntire, T. M., Milton, S. C., Hall, J. E., and Glabe, C. G. (2004) Permeabilization of lipid bilayers is a common conformation-dependent activity of soluble amyloid oligomers in protein misfolding diseases, *J. Biol. Chem. 279*, 46363−46366.
66. Arispe, N. H., Pollard, H. B., and Rojas, E. (1993) Giant multilevel cation channels formed by Alzheimer's disease amyloid β-protein [Aβp-(1−40)] in bilayer membrane, *Proc. Natl. Acad. Sci. U.S.A. 90*, 10573−10577.
67. Quist, A., Doudevsli, I., Lin, H., Azimova, R., Ng, D., Frangione, B., Kagen, B., Ghiso, J., and Lal, R. (2005) Amyloid ion channels: a common structural link for protein-misfolding disease, *Proc. Natl. Acad. Sci. U.S.A. 102*, 10427−10432.
68. Dickson, D. W. (2004) Apoptotic mechanisms in Alzheimer neurofibrillary degeneration: cause or effect, *J. Clin. Invest. 111*, 23−27.
69. Oddo, S., Caccamo, A., Shepherd, J. D., Murphy, M. P., Golde, T. E., Kayed, R., Meterate, R., Mattson, M. P., Akbari, Y., and LaFerla, F. M. (2003) Triple-transgenic model of Alzheimer's disease with plaques and tangles: intracellular Aβ and synaptic dysfunction, *Neuron 39*, 409−421.
70. Lustbader, J. W., Cirilli, M., Lin, C., Xu, H. W., Takuma, K., Wang, N., Caspersen, C., Chen, X., Pollak, S., Chaney, M., Trinchese, F., Liu, S., Gunn-Moore, F., Lue, L.-F., Walker, D. G., Kuppusamy, P., Zeiwier, Z. L., Arancio, O., Stern, D., Yan, S. S., and Wu, H. (2004) ABAD directly links Aβ to mitochondrial toxicity in Alzheimer's disease, *Science 304*, 448−452.
71. Knauer, M. F., Soreghan, B., Burdick, D., Kosmoski, J., and Glabe, C. G. (1992) Intracellullar accumulation and resistance to degradation of the Alzheimer amyloid A4/β protein, *Proc. Natl. Acad. Sci. U.S.A. 89*, 7437−7441.
72. Burdick, D., Kosmoski, J., Knauer, M. F., and Glabe, C. G. (1997) Preferential adsorption, internalization and resistance to degradation of the major isoform of the Alzheimer's amyloid peptide, Aβ1−42, in differentiated PC cells, *Brain Res. 746*, 275−284.
73. Prohaska, J. R., and Gybina, A. A. (2004) Intracellular copper transport in mammals, *J. Nutr. 134*, 1003−1006.
74. Koehler, C. M., Beverly, K. N., and Leverich, E. P. (2006) Redox pathways of the mitochondrion, *Antioxid. Redox Signaling 8*, 813−822.
75. Hiroi, M. A., Tohru, H., Kazuya, H., Masashi, M., Takao, T., and Niki, E. (2005) Regulation of apoptosis by glutathione redox state, *Free Radical Biol. Med. 38*, 1057−1072.
76. Lora, J., Alonso, F. J., Segura, J. A., Lobo, C., Marquez, J., and Mates, J. M. (2004) Antisense glutaminase inhibitions decrease glutathione antioxidant capacity and increase apoptosis, *Eur. J. Biochem. 271*, 4298−4306.
77. Biaglow, J. E., Lee, I., Donahue, J., Held, K., Mieyal, J., Dewhirst, M., and Tuttle, S. (2003) Glutathione depletion or radiation treatment alters respiration and induce apoptosis, *Adv. Exp. Med. Biol. 530*, 153−164.
78. Biroccio, A., Benassi, B., Filomeni, G., Amodei, S., Marchini, S., Chiorino, G., Rotilio, G., Zupi, G., and Ciriolo, M. R. (2002) Glutathione influences C-Myc-induced apoptosis in M14 human melanoma cells, *J. Biol. Chem. 277*, 43763−43770.
79. Van den Dobbelsteen, D. J., Nobel, C. S. I., Schlegel, J., Cotgreave, I. A., Orrenius, S., and Slater, A. F. G. (1996) Rapid and specific efflux of reduced glutathione during apoptosis induced by anti-Fas/APO-1 antibody, *J. Biol. Chem. 271*, 15420−15427.
80. Baloyanis, S. J. (2006) Mitochondrial alterations in Alzheimer's disease, *J. Alzheimer's Dis. 9*, 119−126.
81. Aleard, A. M., Benard, G., Augereau, O., Malgat, M., Talbot, J. C., Mazat, J. P., Letellier, T., Dachary-Prigent, J., Solaini, G. C., and Rossignol, R. (2005) Gradual alteration of mitochondrial structure and function by β-amyloid: importance of membrane viscosity changes, energy deprivation, reactive oxygen species production, and cytochrome *c* release, *J. Bioenerg. Biomembr. 37*, 207−225.
82. Keil, U., Bonert, A., Marques, C. A., Scherping, I., Weyermann, J., Strosznajder, J. B., Mueller-Spahn, F., Czech, C., Pradier, L., Mueller, W. E., and Eckert, A. (2004) Amyloid β-induced changes in nitric oxide production and mitochondrial activity lead to apoptosis, *J. Biol. Chem. 279*, 50310−50320.
83. Ohta, S., and Ohsawa, I. (2006) Dysfunction of mitochondria and oxidative stress in the pathogenesis of Alzheimer's disease, *J. Alzheimer's Dis. 9*, 155−166.
84. Antosh, S. C., and Meduri, A. J. (2006) in U.S. Patent Appl. Publ., pp 10, U.S.

85. Gibson, G. E., Sheu, K. F., and Blass, J. P. (1998) Abnormalities of mitochondrial enzymes in Alzheimer's disease, *J. Neural Transm. 105*, 855−870.
86. de la Monte, S. M., and Wands, J. R. (2006) Molecular indices of oxidative stress and mitochondrial dysfunction occur early and often progress with severity of Alzheimer's disease, *J. Alzheimer's Dis. 9*, 167−181.
87. Zhu, X., Smith, M. A., Perry, G., and Aliev, G. (2004) Mitochondrial failures in Alzheimer's disease, *Am. J. Alzheimer's Dis. Dement. 19*, 345−352.
88. Yan, S. D., Xiong, W.-C., and Stern, D. M. (2006) Mitochondrial amyloid-beta peptide pathogenesis or late-phase development?, *J. Alzheimer's Dis. 9*, 127−137.
89. Moreira, P. I., Cardoso, S. M., Santos, M. S., and Oliveira, C. R. (2006) The key role of mitochondria in Alzheimer's disease, *J. Alzheimer's Dis. 9*, 101−110.
90. Dryhurst, G., Kadish, K. M., Scheller, F., and Renneberg, R. (1982) *Biological Electrochemistry*, Vol. 1, Academic Press, New York and London.
91. Tse, D. C.-S., and Kuwana, T. (1978) *Anal. Chem. 50*, 1315.
92. Conway, B. E. (1969) *Electrochemical Data*, Greenwood Press, New York.
93. Nelson, D. L., and Cox, M. M. (2004) *Lehninger Principles of Biochemistry*, W. H. Freeman, New York.

BI700508N